Study of the influence of internal flow on the spray behavior under cavitating conditions using a transparent nozzle

R. Payri, J. Gimeno[1*], P. Marti-Aldaravi, O. Venegas
CMT-Motores Térmicos, Universidad Politécnica de Valencia, Spain
rpayri@mot.upv.es, jaigigar@mot.upv.es, pedmar15@mot.upv.es and ovenega@mot.upv.es

Abstract

In this paper the behavior of the internal flow under cavitating conditions and its influence on the behavior of the spray is studied. For this purpose, a transparent nozzle (quartz plate) with a cylindrical orifice of sharp entrance and commercial diesel are used. Initially, the nozzle is installed in a pressurized rig with fuel in order to measure the mass flow and observe the flow inside the orifice using a special visualization technique. Since the refractive index of the vapor bubbles of the fuel is different to the refractive index of the fuel in liquid state, the cavitation inside the nozzle can be appreciated. Pressure conditions when the first bubbles inside the orifice appear are compared with the pressure conditions when the flow collapses, showing that the beginning of the cavitation occurs before the mass flow collapse and once the cavitation is fully developed through the whole orifice the mass choke occurs.

Following, using the same visualization technique and pressurizing the rig with air it is possible to visualize the spray and link it with the appearance of cavitation inside the orifice. It is observed that the cavitation has an influence on the cone angle in the first millimeters and the distance between peaks of two consecutive points of the oscillatory contour of the spray.

Introduction

Over the last years the study of the sprays in diesel engines has become very important because of the effect the spray atomization and the air-fuel mixture have on the combustion efficiency and pollutant formation.

As a result of these studies, several tools have been developed for analyzing and modeling macroscopic spray behavior [1]-[6]. Nevertheless, there are still uncertainties related with the internal nozzle flow and its link with spray formation and primary break-up because the small geometries of the nozzle orifices and the high velocities of the flow inside them make difficult the study of the physics of this phenomenon, especially when hydrodynamic cavitation appears. Traditionally, hydraulic criterion to detect the existence of cavitation, based on the start of mass flow choking, has been used. Other researches [7]-[15] point to the visualization of the flow inside the nozzle with the goal to observe the cavitation phenomenon and its influence in the spray development. In these researches different nozzle models have been developed with optical materials that allow the visualization inside the hole such as quartz and methacrylate. However, a few studies made with transparent orifices revealed that cavitation bubbles appear at less critical conditions and that cavitating conditions affect the spray behavior [14],[15].

The goal of this paper is to study the influence of cavitation on near-nozzle spray characteristics using a transparent nozzle (quartz-fused silica, SiO_2) with a cylindrical orifice. For this purpose hydraulic characterization in terms of mass flow is made filling the discharge chamber with the same liquid that is injected, finding the pressure conditions where mass flow is choked and allowing to visualize simultaneously the bubbles present both inside and at the exit of the orifice under cavitating conditions. This way, the images can be compared with hydraulic characterization results in order to know what happens inside the orifice when the flow collapses.

For visualization, a special optical system and flash (white light) backlighting has been developed to focus a window size of 3 mm (around 500 pixel/mm) that allows seeing the flow inside the orifice and a portion of the spray at the exit (first 1.5 mm of the spray).

Finally, using the same visualization technique, the discharge chamber is pressurized with air under the same conditions than when it was filled with fuel and is used in order to link the previous cavitation analysis with the behavior of the spray in the near-nozzle field at stationary conditions.

* Corresponding author: jaigigar@mot.upv.es

This paper is structured in four sections. First, a review of the concepts used in the calculation and definition of the cavitation and internal flow in nozzles is made; introducing several important parameters that will be used in the rest of the study. Second, the experimental facilities and methodology are described, paying special attention to the optical system for internal flow visualization. In the third section the results from hydraulic characterization and internal flow visualization are presented and analyzed, showing the evolution of the cavitation and its influence on the spray behavior. In the last section some general conclusions will be established.

Theoretical Background

In a diesel injector nozzle, high velocities at the orifice inlet due to the abrupt change of section and flow direction tend to separate the boundary layer from the wall. As a consequence, a recirculation phenomenon appears in this zone (Figure 1), accompanied by a pressure fall due to the acceleration of the fluid. If conditions in recirculation zone are such that static pressure falls under vapor pressure of the working fluid, local change of state from liquid to vapor takes place. This phenomenon is called cavitation.

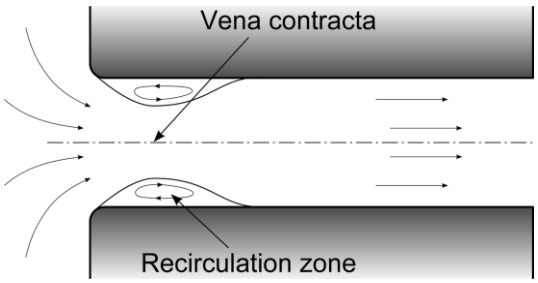

Figure 1 Flux lines at the inlet of the nozzle for an axi-symmetric nozzle.

As a consequence of the complexity to obtain information about the behavior of the flow inside the orifice in real nozzles, non-intrusive techniques have been developed to determine the appearance of the cavitation. One of the criteria often used to determine the appearance of the cavitation is the one proposed by Nurick [16], where the mass flow obtained in stationary conditions increases as a linear function of the square root of the pressure drop until a point where it stabilizes due to the cavitation phenomena. At this point, the so called "choked flow" occurs and pressure conditions needed to achieve it are named *critical cavitation conditions* (Figure 2).

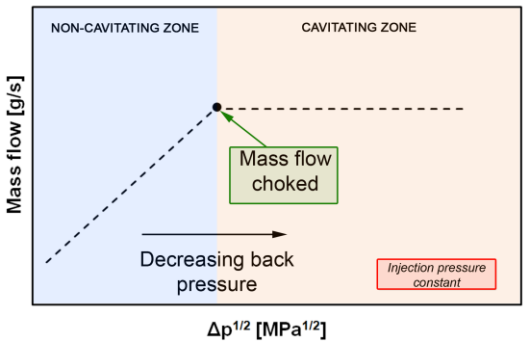

Figure 2 Mass flow rate tendency in cavitating nozzles ($\Delta p = p_{inj} - p_{back}$).

The cavitation number (K) is defined by Nurick (Equation (1)). This K increases as the injection pressure (p_{inj}) decreases or when the discharge pressure downstream the orifice (p_{back}) increases. p_v is the vapor pressure of the fuel. As the cavitation number (K) is smaller, the tendency to cavitate is higher.

$$K = \frac{p_{inj} - p_v}{p_{inj} - p_{back}} \qquad (1)$$

This way mass flow choking is an indirect method to predict at which conditions the cavitation appears in a nozzle. However, other authors have tried to go one step further in understanding the phenomenon of cavitation and its appearance inside the orifice. For most of these researches several models for transparent nozzles at large scale have been used [7]-[11], others have used geometries at smaller scale but without keeping up the exact geometry of a real nozzle [2], [17], [18] and very few have performed studies in nozzles at small scale and/or with reproducible geometry [19]. Some of these studies, along with others where transparent nozzles have not been used [20], [21] have demonstrated that cavitation inception detected by visualizing bubbles in the nozzles is not coincident with the collapse of mass flow.

Experimental Methods

To carry out the hydraulic characterization of the nozzle and flow visualization inside it, a rig as the one shown in Figure 3 has been used. This rig consists of a stainless steel vessel, including two opposed optical windows, so that backlighting visualization can be performed. The upper cap allows the fuel supply and is adapted to contain the transparent nozzle. The bottom cap includes the backpressure regulation system.

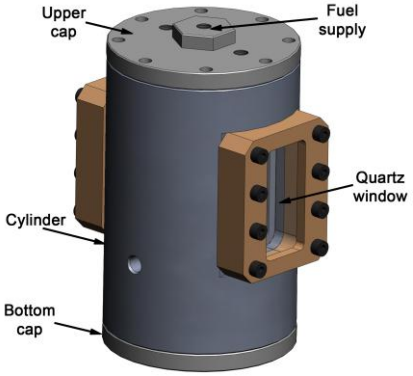

Figure 3 Visualization test rig.

The transparent nozzle is made of fused silica SiO_2 and has an orifice with exit diameter of 510 µm, 1 mm length and sharp entrance (Figure 4). For the assembly of the nozzle in the rig, a holding system has been developed as shown in Figure 5. It consists of an upper cap coupled directly to the rig cylinder and allows the fuel supply; besides it has a lower piece called "base" that allows the entry of light for flow visualization and finally it has a large size nut which couples the two pieces (upper cap and base). The transparent nozzle is located in the middle of the upper cap and the base and is separated by expanded graphite laminated gaskets to prevent fuel leakage and local strains over quartz surfaces in contact that may lead to a breakage of the nozzle.

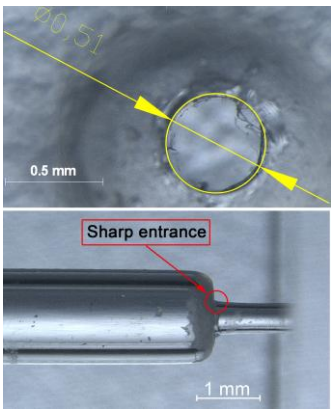

Figure 4 Transparent nozzle images obtained with microscope.

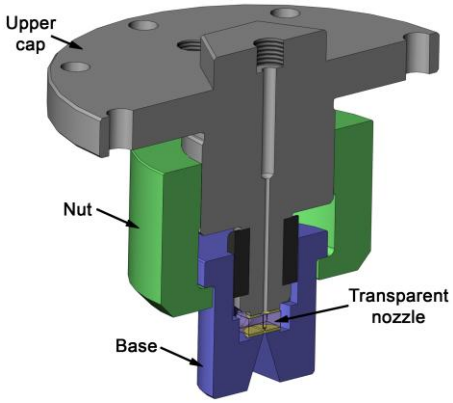

Figure 5 Holding system for the transparent nozzle.

Tests performed are divided in two stages: first, creating pressure in the chamber with the same fuel that will be injected in order to perform the hydraulic characterization and visualize the bubbles in the spray. The second stage consists in generating the backpressure with air to visualize the spray at the exit of the nozzle. The fuel used is commercial diesel fuel and Table 1 presents a summary of the properties considered in this study; as it is shown, the fuel has a refractive index close to the quartz refractive index which is 1.461 at a wavelength of 532 nm [22], [23], making easier the visualization inside the orifice.

Density$_{@40°C}$ [Kg/m3]	Viscosity$_{@40°C}$ [cSt]	Vapor pressure$_{@40°C}$ [MPa]	n$_{@532nm}$ [-]
826.44	2.6	Negligible	1.457

Table 1 Physical properties of the commercial diesel.

Hydraulic characterization

Hydraulic characterization is done by measuring the mass flow of the nozzle injecting fuel at stationary conditions. For this purpose, the test rig is filled with fuel and the nozzle injects in continuous flow. A needle-valve

placed at the test rig exit regulates the pressure inside it and is in turn connected to a multiway valve with one entry and two exits. Once the target chamber pressure is reached, the multiway valve is set to direct the flow towards the gravimetric balance. Since the mass flow at the exit of the rig is the same as the flow through the orifice, the stationary mass flow can be calculated for a given time. Mass flow is measured for different injection pressures (3, 6, 9 and 12MPa) and for each injection pressure the backpressure increases starting at cavitating conditions and until the flow stops cavitating. Figure 6 shows a diagram of the assembly used for the measures of mass flow in continuous (permeability).

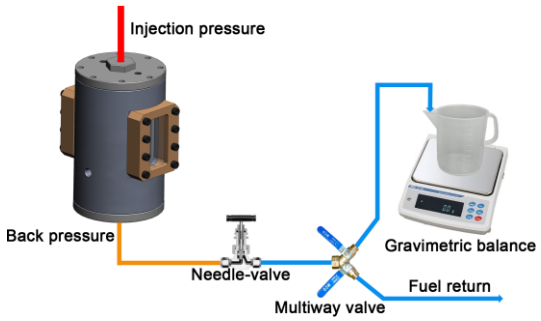

Figure 6 Scheme for the hydraulic characterization.

Internal flow visualization

The optical system developed for visualization includes one optical fiber, a PCO SensiCam CCD Camera and one optical lens with a focal length of 100 mm, aligned between each other in order to reach high zoom levels. These elements are placed in a three-axis coordinate system. This configuration allows fixing distances between test rig, focal lens and camera so that visualization window and zoom level can be adapted to the objective of the experiments and in function of the window size.

Additionally, an optical diffuser is placed after the light flash exit. This element diffuses the flash light and produces a uniform illumination in the chamber region under study. Figure 7 shows a diagram of the acquisition system used for visualization.

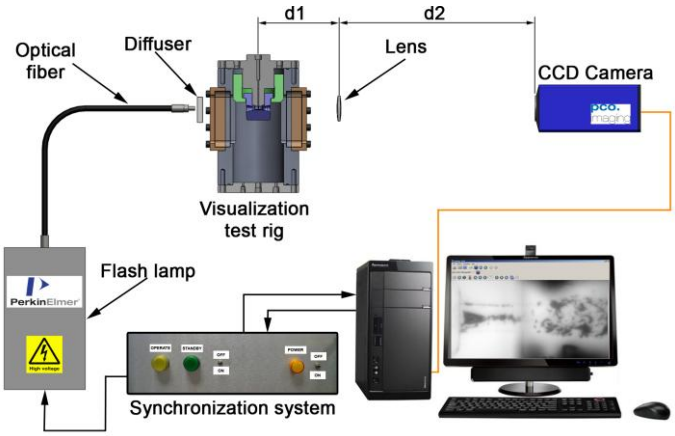

Figure 7 Scheme of the synchronization system.

The optical path length changes with the refractive index of the medium. Since two different fluids have been used to generate the backpressure in the test rig (liquid fuel, in order to visualize cavitation bubbles that exit the nozzle, and air to analyze spray behavior), the distance from the quartz plate to the lens needs to be adjusted depending on the fluid in the chamber (Figure 7). Table 2 provides information about optical distances for the two configurations used for a window size of 3mm (around 500 pixel/mm).

Medium	$n_{@532nm}$ [-]	d1 [mm]	d2 [mm]
Fuel	1.457	162	417
Air	1.000	144	417

Table 2 Optical distances for the two configurations used.

At the same time hydraulic characterization is made (injecting on fuel), the images of the flow inside the orifice and the bubbles in the spray in the first millimeters are obtained using diffused backlighting illumination. Due to the difference in refractive index between liquid and vapor phase, only bubbles inside the orifice and those coming out of it are visualized. The same discharge pressures intervals for each injection pressure from hydraulic characterization are used and 20 images per test condition are taken. However, for visualization tests some additional backpressure values are added in order to obtain images of the cavitation appearance and its development inside the orifice.

Additional measurements are carried out in the test rig pressurizing with air to observe the spray at the outlet orifice using the same measurement conditions, visualization technique and resolution (around 500 pix/mm). This configuration allows determining the correspondence between the behavior of the flow inside the orifice and the spray at the exit in the first millimeters. Besides, images injecting on air provide the cavitating contour of the spray and also give information about the behavior of the flow on those first millimeters, as cone angle which is calculated by applying a linear fit to the points belonging to the boundary detected for each one of the two sides of the contour and the characteristic distance between peaks (*Dp*), that can be obtained as an average value of the distance between two consecutive local maximums of the detected contour [21].

All images are obtained at an exposure time of 500 ns and in order to detect better the cavitating zones inside the orifice as well as bubbles in the spray at the exit of the orifice. The images obtained are posteriorly processed with a custom-made algorithm. This function allows matching in position each image with respect to the background; which is later subtracted.

Results and Discussion

Hydraulic Characterization

Knowing the nozzle geometry through the images taken on the microscope (Figure 4), the measures of mass flow rate were made under stationary conditions at different backpressure values keeping injection pressure constant (3, 6, 9 and 12MPa). By applying a linear fit and calculating the intersection with the value of mass flow after choking, critical conditions can be obtained [24]. This information is shown in the Figure 8 and the values of critical cavitation number (K_{crit}) for each injection pressure are tabulated in Table 3.

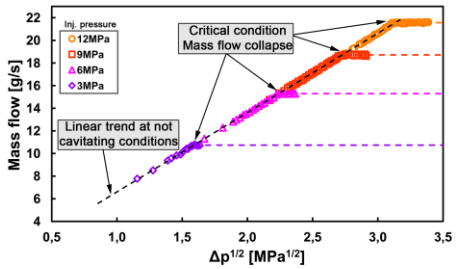

Figure 8 Mass flow behavior.

p_{inj} [MPa]	$\Delta p_{crit}^{1/2}$ [MPa$^{1/2}$]	K_{crit} [-]
3	1.59	1.08
6	2.24	1.13
9	2.75	1.14
12	3.11	1.21

Table 3 Critical cavitation number for each injection pressure.

In Figure 8 can be observed that the mass flow choked for each injection pressure occurs at different values of the square root of the pressure drop ($\Delta p_{crit}^{1/2}$). Under non-cavitating conditions the tendency of the mass flow is linear to the root of the pressure drop and follows the same tendency line for all injection pressures. However, the mass flow collapse occurs at more critical conditions as the injection pressure increases.

Internal flow visualization

Figure 9 shows the cavitation inside the orifice and the bubbles in the spray at the exit (dark zone in the middle of the image). Being a circular orifice instead of flat as in other studies [12], the image shows the cavitation around the whole wall of the orifice. Thus the cavitation observed in the central part of the orifice represents the cavitation from both the front and back of the orifice.

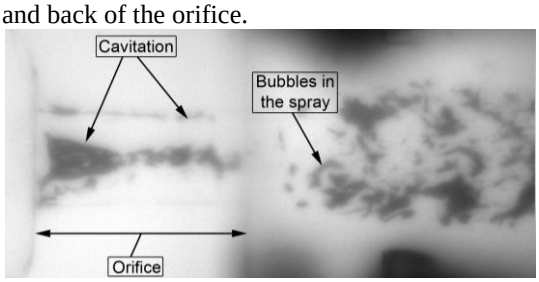

Figure 9 Image under cavitation conditions at p_{inj} =3 MPa and p_{back} =0.2 MPa (injecting on fuel).

Figure 10 shows the evolution of cavitation for the injection pressure of 3MPa.When comparing the results of hydraulic characterization with those from visualization, it is observed that the incipient cavitation occurs at a pressure differential lower than when the mass flow collapse occurs (1.42 $MPa^{1/2}$ < 1.59 $MPa^{1/2}$) or at higher cavitation numbers (1.38 > 1.08); which confirms the results obtained in other studies [20], [21]. Another fact of great interest is that the mass choke occurs once the cavitation has extended until the exit of the orifice.

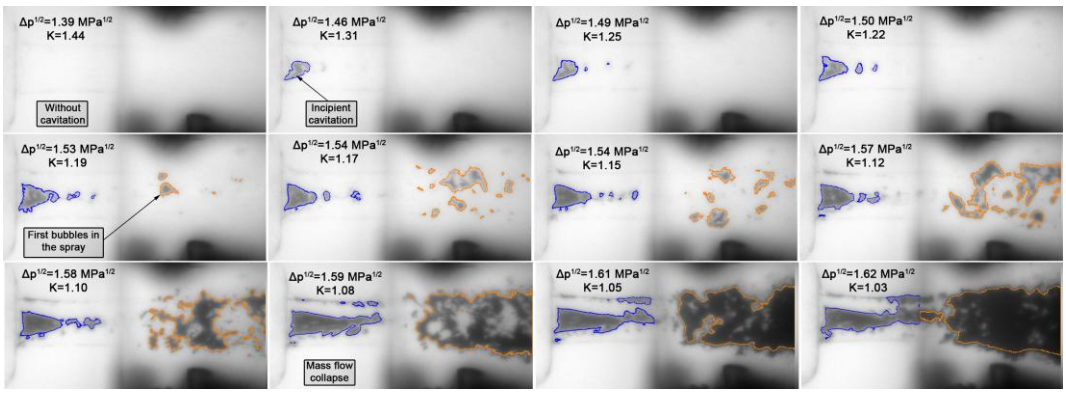

Figure 10 Evolution of cavitation at p_{inj} =3 MPa and different discharge pressures.

The same occurs for all injection pressures and in Table 4 the new critical values are summarized, taking as criterion the incipient cavitation obtained from the images. These values have the subscript v, indicating that they have been found using the visualization technique.

p_{inj} [MPa]	$\Delta p_{crit-v}^{1/2}$ [$MPa^{1/2}$]	K_{crit-v} [-]
3	1.46	1.31
6	2.02	1.41
9	2.35	1.58
12	2.62	1.71

Table 4 Critical cavitation number with incipient cavitation criterion.

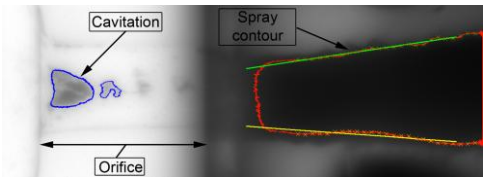

Figure 11 Image injecting on air. p_{inj} =3 MPa and p_{back} =0.4 MPa.

The final step is to visualize the near-nozzle spray on an air pressurized atmosphere (Figure 11) in order to link the previous cavitation analysis with the behavior of the spray at stationary conditions. Below, spray visualization results obtained and compared with the tests in liquid environment are shown for the pressures of 3 y 6 MPa. It was not possible to perform tests at 9 and 12 MPa injecting on an air pressurized atmosphere because the windows of the rig get dirty very quickly preventing the visualization.

Spray visualization results obtained for the injection pressures of 3 and 6 Mpa are shown in Figure 12. In this figures, the evolution of the spray cone angle in the first millimeters with respect to cavitation number (K) is represented together with sample images of different conditions injecting on liquid (superior) and air (inferior). Particularly, three scenarios are shown from left to right for each injection pressure: when bubbles first appear in the spray, when the incipient cavitation is observed and a condition without cavitation.

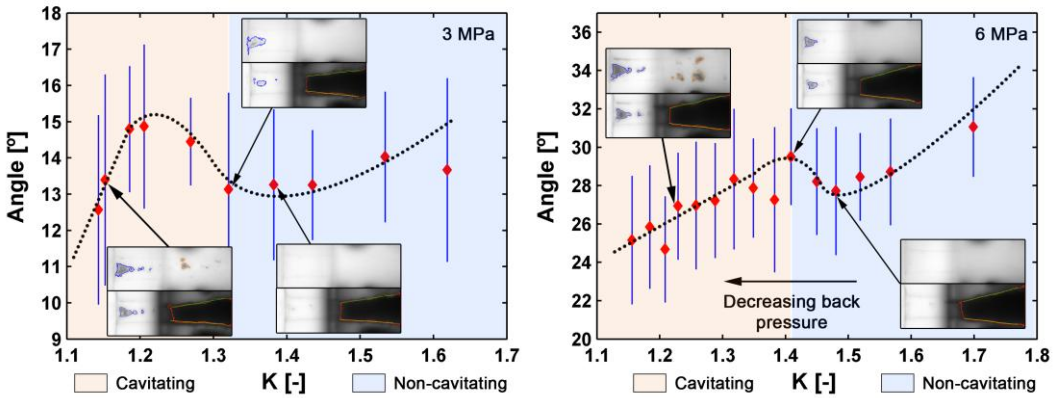

Figure 12 Spray cone angle in the first millimeters respect to cavitation number.

As it can be seen in Figure 12, when decreasing the back pressure (moving to the left side of the figure), the spray cone angle decreases due to the effect of chamber density, as expected from previous analysis [4], [25]. This trend continues until reaching the pressure conditions at which incipient cavitation is visualized (K_{crit-v}). At this point, the spray angle shows a significant increment. If the backpressure keeps decreasing, the effect of cavitation stabilizes, and chamber density recovers its original influence. The same behavior is seen for the two pressure conditions.

Together with the spray cone angle, Figure 13 shows that the distance between peaks gets appreciably lower when cavitation incipient is detected inside the orifice with respect to the non-cavitating situation. This can be considered as an increase of the level of irregularities in the spray contour and it can be established as an indicator of the turbulence at the nozzle exit.

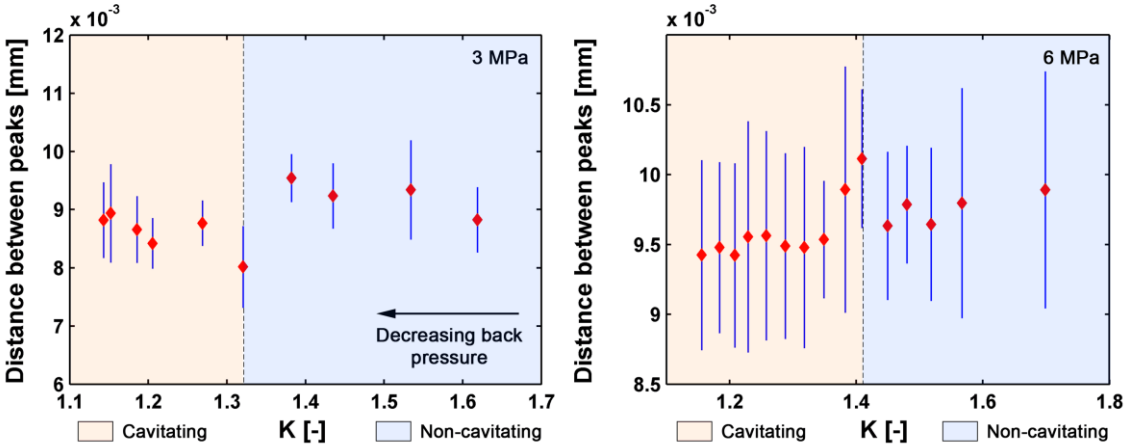

Figure 13 Distance between consecutive peaks of boundary oscillations against K.

On the other hand, in contrast to previous studies [20], [21], and as a major contribution to the field of study, the influence of the cavitation inside the orifice on the spray behavior in the first millimeters could be observed. On those studies the influence of the cavitation is linked only with the formation of bubbles on the spray which, as has been observed, occurs at more critical conditions that incipient cavitation.

Summary and Conclusions

The aim of this paper was to visualize the flow inside the orifice and the near-nozzle spray on a liquid and air pressurized atmospheres, in order to link the cavitation inside the orifice and the formation of bubbles in the spray with the behavior of the spray at stationary. For this purpose special near-nozzle field visualization applying backlighting technique in a pressurized chamber (both with air and fuel) has been used.

After performing the hydraulic characterization and visualization of the transparent nozzle, several conclusions have been obtained:

- Mass flow choked has been compared with the incipient cavitation shown in visualization tests. In terms of K, the cavitation detection by the optical procedure has shown higher values than those found in mass flow choked. This effect could be due to the fact that there has to exist a big amount of bubbles in the exit section for the mass flow collapse to occur.
- It could be observed that the flow collapse occurs right when cavitation is fully developed in the orifice. Also, that the first bubbles in the spray appear before the mass choked.
- An increase of the stationary spray cone angle in the first millimeters is observed at the same pressure conditions at which incipient cavitation appear inside the orifice. This increment in the spray cone angle has been observed changing cavitation regime by different values of chamber pressure.
- Additionally, an analysis of oscillations in the spray boundary has been carried out, showing a decrease of the mean distance between consecutive peaks when cavitation appears in the orifice.
- Finally, the results obtained have been compared to those found in previous studies. In contrast to them, it was possible to study the influence of the cavitation from incipient cavitation inside the orifice and not only based on the formation of bubbles in the spray, highlighting that the changes both in the cone angle and the distance between peaks occur when the cavitation inside the orifice appears.

Acknowledgements

The authors would like to José Enrique del Rey* for his collaboration in the experimental measurements. This work has been funded by Universidad Politécnica de Valencia from Spain, in the framework of the project "*Estudio de la influencia del levantamiento de aguja en el proceso de inyección Diesel*", Reference No. PAID-06-10-2362. (*) From CMT-Motores Térmicos. Universidad Politécnica de Valencia.

References

[1] Soteriou, C., Smith, M., Andrews, R., 1995. Direct injection diesel sprays and the effects of cavitation and hydraulic flip on atomization. *SAE Paper 950080* (1995).

[2] Hiroyasu, H., Spray breakup mechanism from the hole-type nozzle and its applications. *Atomization and Sprays* 10, 511–527 (2000).

[3] Lee, C.S., Lee, K.H., Reitz, R.D., Park, S.W., Effect of split injection on the macroscopic development and atomization characteristics of a diesel spray injected through a common-rail system. *Atomization and Sprays* 16 (5), 543–562 (2006).

[4] Hiroyasu H, Arai, A. Structures of fuel sprays in Diesel engines. SAE Paper 900475; 1990.

[5] Desantes JM, Payri R, Salvador FJ, Gil A. Development and validation of a theoretical model for diesel spray penetration. Fuel 2006; 85:910–7.

[6] Sou, A., Hosokawa, S., Tomiyama, A., 2007. Effects of cavitation in a nozzle on liquid jet atomization. *International Journal of Heat and Mass Transfer* 50, 3575–3582.

[7] Oda, T.; Goda, Y.; Kanaike, S.; Aoki, K. & Ohsawa, K. Experimental Study about internal Cavitating Flow and Primary Atomization of a Large-Scaled VCO Diesel Injector with Eccentric Needle. *11th Triennial International Annual Conference on Liquid Atomization and Spray Systems*, 2009, 132.

[8] Chaves H., Knapp M., Kubitzek A., and Obermeier F., Experimental Study of Cavitation in the Nozzle Hole of Diesel Injectors Using Transparent Nozzles, *SAE Paper No. 950290*, 1995.

[9] Chaves H., Kirmse C., and Obermeier F. The Influence of Nozzle Inlet Curvature on Unsteady Cavitation in Transparent Diesel Injection Nozzles, *1st International Colloquium on Microhydrodynamics*, Paris, 2000.

[10] Arcoumanis, C., M. Badami, H. Flora, and M. Gavaises, Cavitation in Real-Size Multi-Hole Diesel Injector Nozzles. *SAE Paper 2000-01-1249*, 2000.

[11] Walther J., Schaller J.K., Wirth R., Tropea C., Investigation of internal flow in transparent diesel injection nozzles using fluorescent particle image velocimetry (FPIV), *Proc. ICLASS 2000* (2000).

[12] Sou, A. Tomiyama, A. Hosokawa, S. Nigorikawa, S. Maeda, Cavitation in a Two-Dimensional Nozzle and Liquid Jet Atomization, *JSME International Journal Series B*, 2006.

[13] Ganippa L.C., Bark G., Andersson S., Chomiak J., Comparison of cavitation phenomena in transparent scale-up single-hole diesel nozzles, *Proc. CAV2001* (2001) A9.005.

[14] Winklhofer, E., Kull, E., Kelz, E., Morozov, A., 2001. Comprehensive hydraulic and flow field documentation in model throttle experiments under cavitation conditions. *ILASS-Europe 2001*, Zurich, 2–6 September 2001.

[15] Mishra, C., Peles, Y., 2005. Cavitation in flow through a micro-orifice inside a silicon microchannel. *Physics of fluids* 17, 013601.

[16] Nurick, W.H., 1976. Orifice cavitation and its effect on spray mixing. *ASME Journal of Fluids Engineering* 222, 681–687.

[17] Ganippa, L.C., Bark, G., Andersson, S., Chomiak, J., Cavitation: a contributory factor in the transition from symmetric to asymmetric jets in cross flow nozzles. *Experiments in Fluids* 36, 627–634 (2004).

[18] Suh, H.K., Lee, C.S., 2008. Effect of cavitation in nozzle orifice on the diesel fuel atomization characteristics. *International Journal of Heat and Fluid Flow* 29 (4), 1001–1009.

[19] Blessing, M.; König, G.; Krüger, C.; Michels, U. & Schwarz, V. Analysis of flow and cavitation phenomena in diesel injection nozzles and its effects on spray and mixture formation *SAE Paper 2003-01-1358, Society of Automotive Engineers*, Inc., Warrendale, Pennsylvania, USA, 2003.

[20] Payri, R., F.J. Salvador, J. Gimeno, J. de la Morena, 2009. Study of cavitation phenomena based on a technique for visualizing bubbles in a liquid pressurized chamber. *International Journal of Heat and Fluid Flow* 30 (2009) 768–777.

[21] Desantes, J.M., Payri, R., Salvador, F.J., De la Morena, J., 2010. Influence of cavitation phenomenon on primary break-up and spray behavior at stationary conditions. *Fuel* 89 (2010) 3033–3041.

[22] H. Malitson, "Refractive Index of Fused Silica," *J. Opt. Soc. Am.* 55, 1205 (1965).

[23] Ghosh G., Handbook of Thermo-Optic Coefficients of Optical Materials with Applications Academic, San Diego, Calif., 1997.

[24] Payri, F., Bermúdez, V., Payri, R., Salvador, F.J., 2004a. The influence of cavitation on the internal flow and the Spray characteristics in diesel injection nozzles. *Fuel* 83, 419–431.

[25] Payri R, Salvador FJ, Gimeno J, Soare V. Determination of diesel spray characteristics in the real engine in-cylinder air density and pressure conditions. *J Mech Sci Technol* 2005; 19(11):2040–52.